AD-A146 284 THE EFFECT OF THIN-FILM GROWTH MODE ON XPS/UPS/AES 1/1
INTENSITIES. . (U) AEROSPACE CORP EL SEGUNDO CA CHEMISTRY
AND PHYSICS LAB P A BERTRAND 27 AUG 84
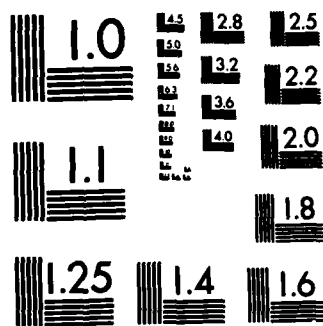UNCLASSIFIED TR-0084(4945-06)-4 SD-TR-84-32 F/G 7/4 NL

END
FILMED
DTIC

MICROCOPY RESOLUTION TEST CHART

AD-A146 284

The Effect of Thin-Film Growth Mode
on XPS/UPS/AES Intensities

P. A. BERTRAND
Chemistry and Physics Laboratory
Laboratory Operations
The Aerospace Corporation
El Segundo, Calif. 90245

27 August 1984

DTIC
ELECTE
S OCT 1 1984
q^c B

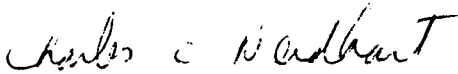**APPROVED FOR PUBLIC RELEASE;**
DISTRIBUTION UNLIMITED

84 33 24 046

Charles C. Neidhart, Lt, USAF
Project Officer

Joseph Hess, GM-15, Director, West Coast
Office, AF Space Technology Center

SECURITY CLASSIFICATION OF THIS PAGE (When Data Entered)

REPORT DOCUMENTATION PAGE	READ INSTRUCTIONS BEFORE COMPLETING FORM
1. REPORT NUMBER SD-TR-84-32	2. GOVT ACCESSION NO. AD-A146284	3. RECIPIENT'S CATALOG NUMBER

4. TITLE (and Subtitle) THE EFFECT OF THIN-FILM GROWTH MODE ON XPS/UPS/AES INTENSITIES	5. TYPE OF REPORT & PERIOD COVERED
	6. PERFORMING ORG. REPORT NUMBER TR-0084(4945-06)-4

7. AUTHOR(s) Patricia A. Bertrand	8. CONTRACT OR GRANT NUMBER(s) F04701-83-C-0084

9. PERFORMING ORGANIZATION NAME AND ADDRESS The Aerospace Corporation El Segundo, Calif. 90245	10. PROGRAM ELEMENT, PROJECT, TASK AREA & WORK UNIT NUMBERS

11. CONTROLLING OFFICE NAME AND ADDRESS Space Division Los Angeles Air Force Station Los Angeles, Calif. 90009	12. REPORT DATE 27 August 1984
	13. NUMBER OF PAGES 29

14. MONITORING AGENCY NAME & ADDRESS(if different from Controlling Office)	15. SECURITY CLASS. (of this report) Unclassified
	15a. DECLASSIFICATION/DOWNGRADING SCHEDULE

16. DISTRIBUTION STATEMENT (of this Report)

Approved for public release; distribution unlimited.

17. DISTRIBUTION STATEMENT (of the abstract entered in Block 20, if different from Report)

18. SUPPLEMENTARY NOTES

19. KEY WORDS (Continue on reverse side if necessary and identify by block number)

AES
Deposition
Thin films
UPS
XPS

20. ABSTRACT (Continue on reverse side if necessary and identify by block number)

The growth mode of thin-film deposition must be taken into account when one assesses surface electron spectroscopy data for evidence of interdiffusion of deposited and substrate material. Three models of thin-film growth are examined for their influence on signal intensity: layer-by-layer growth and two different island-growth mechanisms. Island growth, in which islands of a fixed lateral dimension first grow to a given height and then spread to

DD FORM 1473 (FACSIMILE)

19. KEY WORDS (Continued)

20. ABSTRACT (Continued)

cover the surface, was found to fit available UPS (ultraviolet photoelectron spectroscopy) data on the deposition of Ag on Ge. More data, such as transmission electron micrographs verifying deposit growth mode or UPS valence band changes indicating Ag-Ge interactions, must be obtained before conclusions concerning diffusion vs. island formation can be made.

CONTENTS

Accession For

NTIS CRA&I

DTIC TAB

Unannounced

Justification

Distribution/

Availability Codes

Avail and/or

Dist   Special

A-1

1

FIGURES

I. INTRODUCTION

The deposition of thin films is a widespread manufacturing technique, particularly in the electronics industry. The mode of deposit growth can be important to the final properties, particularly for very thin films. First, if the depositing material reacts with the substrate, a diffuse interfacial region with properties different from those of either the deposit or the substrate may be formed. Second, very thin films may not be continuous if growth occurs by nucleation and island formation rather than by a layer-by-layer mechanism. The growth mode followed in a particular system is affected by many parameters, such as deposition temperature, deposition rate, the chemical reactivities of deposit and substrate, and so on.

The surface electron spectroscopies (XPS, or x-ray photoelectron spectroscopy; AES, or Auger electron spectroscopy; and UPS, or ultraviolet photoelectron spectroscopy) have been used to deduce the interfacial structure of very thin films by following the variation in intensity of substrate and deposit signals as a function of the amount of material deposited. However, unsubstantiated conclusions have been drawn because of a lack of understanding of the effect of growth modes, particularly island growth, on these intensity changes. Growth is generally assumed to be layer by layer, and experimental results that differ from the predictions of this model are assigned to substrate-deposit interdiffusion.

For example, Rossi et al.[1] studied the deposition of silver (Ag) on germanium (Ge) by using UPS from a synchrotron radiation source. They found that the signal intensity for the substrate did not fall as rapidly as expected for layer-by-layer growth of the deposit, and the signal intensity for the deposit did not rise as rapidly as expected. Therefore, they deduced that there was interdiffusion of Ag and Ge at the interface. Ludeke[2] later pointed out that island growth could also produce these effects, and introduced a two-step growth model to illustrate the deviation from layer-by-layer behavior possible for a simple model of island growth. In the first step of this model, islands form and grow laterally and perpendicularly to the surface

at the same rate until they coalesce. In the second step, growth is layer by layer. The model predictions were never compared directly to the experimental data.

In this paper, a more realistic model of island growth will be examined, in which growth occurs in three steps. In the first step, islands of a given lateral size are nucleated and grow only perpendicularly to the surface until a limiting height is reached. In the second step, the islands grow laterally until they coalesce. In the third step, growth is layer by layer. This three-step growth mode has been observed in layers grown by nondeposition methods, such as in the anodic oxidation of gallium arsenide (GaAs).[3] The results of this model will be compared with those of the two-step model, and finally both models' predictions will be compared with the experimental data.

II. DEPOSIT-GROWTH MODELS

A. ONE-STEP GROWTH

The simplest form of deposit growth is one-step growth, in which the deposit forms layer by layer (Fig. 1a). This is the growth mode usually assumed when electron spectroscopic results are assessed. The variation in substrate intensity is well known to be[4]

$$\frac{I(sub)}{I_0(sub)} = \exp\left(-\frac{s}{\lambda \sin\alpha}\right) \tag{1}$$

where $I_0(sub)$ is the signal intensity for the clean substrate, s is the thickness of the overlayer, λ is the escape depth of the electrons being measured, and α is the detection angle. The variation in deposit intensity is[4]

$$\frac{I(dep)}{I_0(dep)} = 1 - \exp\left(-\frac{s}{\lambda \sin\alpha}\right) \tag{2}$$

$I_0(dep)$ is the signal intensity for an infinitely thick deposit.

B. TWO-STEP GROWTH

A model of nucleated deposit growth, in which islands form and then grow at the same rate both laterally and perpendicularly to the surface, has been proposed by Ludeke.[2] He assumes that all impinging and adsorbed atoms migrate to the island nuclei and become part of them; no new island nuclei form. This growth mode is illustrated in Fig. 1b. The islands will coalesce at some vertical dimension t_0. The initial number of islands per unit area ρ will determine the value of t_0: $t_0 = 1/\sqrt{\rho}$. After coalescence, the second-step growth mode is assumed to be layer by layer. The average thickness s of the deposit is defined as the thickness the deposit would have for layer-by-layer growth. Thus the average thickness will be smaller than the thickness of the islands until coalescence occurs.
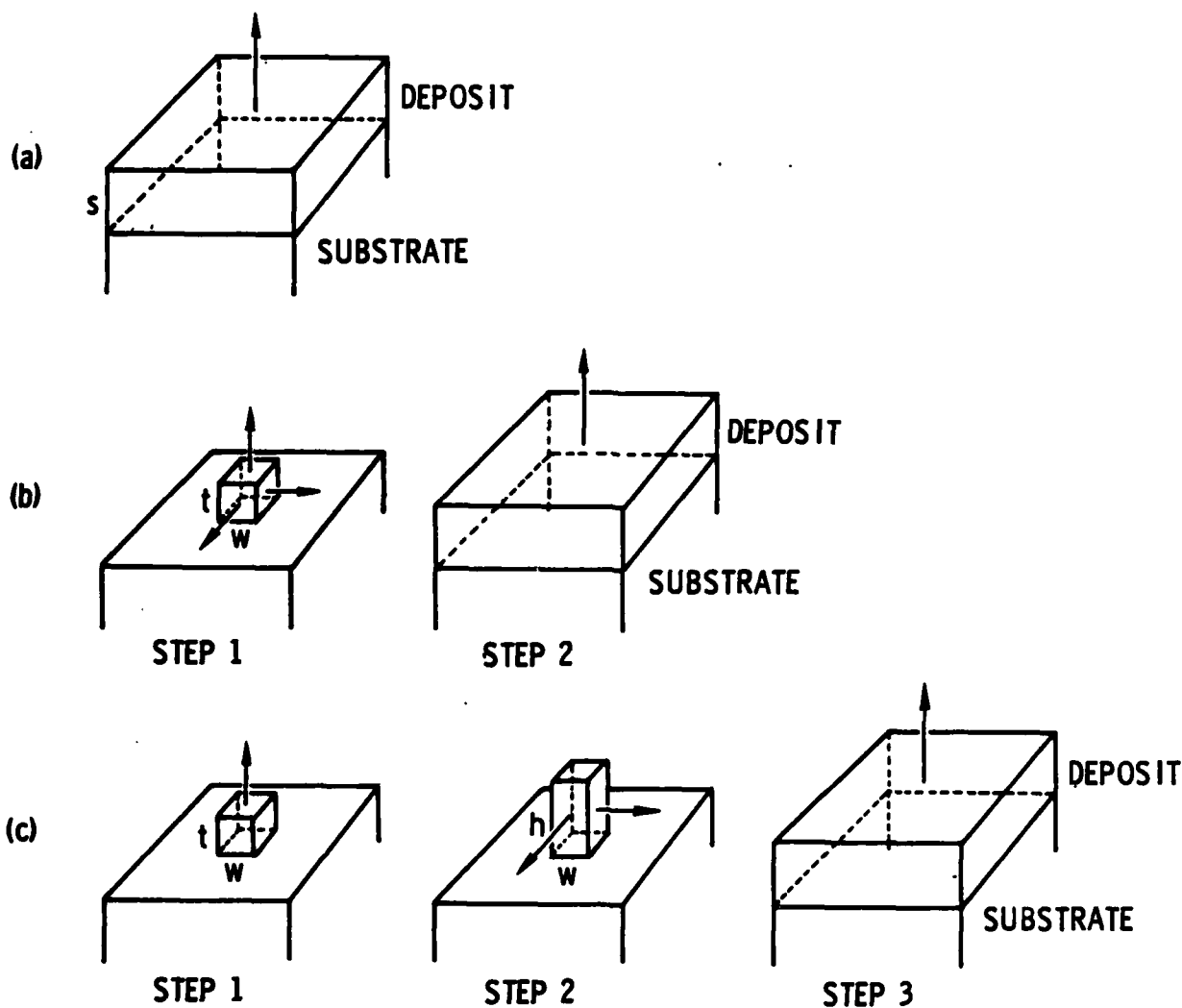
5

Fig. 1. Schematic Illustrations of Deposit Growth Models.
(a) One-step growth model in which deposit grows layer by
layer. (b) Two-step growth model in which island growth
perpendicular to the surface occurs at the same rate as
lateral island growth. (c) Three-step growth model in
which islands of a fixed lateral dimension first grow to
a given height and then spread laterally.

6

Mathematically, then, for the first step ($0 < s < t_0$), we have

$$\frac{I(\text{sub})}{I_0(\text{sub})} = \frac{I}{I_0} \text{ (covered region)} + \frac{I}{I_0} \text{ (uncovered region)} \qquad (3)$$

For any given s, the area A that is covered by deposited material per unit area of substrate can be calculated. Letting w be the lateral dimension of an island and t its thickness, we know that $w = t$ and $s = tw^2\rho$. So

$$A = w^2\rho = \left(\frac{t}{t_0}\right)^2 = \left(\frac{s}{t_0}\right)^{2/3} \qquad (4)$$

Thus the intensity ratio becomes

$$\frac{I(\text{sub})}{I_0(\text{sub})} = \left(\frac{s}{t_0}\right)^{2/3} \exp\left[\frac{\left(st_0^2\right)^{1/3}}{\lambda\sin\alpha}\right] + \left[1 - \left(\frac{s}{t_0}\right)^{2/3}\right]$$

$$= 1 + \left(\frac{s}{t_0}\right)^{2/3} \left\{\exp\left[-\frac{\left(st_0^2\right)^{1/3}}{\lambda\sin\alpha}\right] - 1\right\} \qquad (5)$$

After coalescence, during layer-by-layer growth ($s > t_0$)

$$\frac{I(\text{sub})}{I_0(\text{sub})} = \exp\left(-\frac{s}{\lambda\sin\alpha}\right) \qquad (6)$$

The signal intensity ratio for the deposit can be similarly calculated. For the first step, island growth ($0 < s < t_0$),

$$\frac{I(\text{dep})}{I_0(\text{dep})} = \frac{I}{I_0} \text{ (covered)}$$

$$= \left(st_0^2\right)^{2/3} \left\{1 - \exp\left[-\frac{\left(st_0^2\right)^{1/3}}{\lambda\sin\alpha}\right]\right\} \qquad (7)$$

7

and for the second step $(s > t_0)$

$$\frac{I(dep)}{I_0(dep)} = 1 - \exp\left(- \frac{s}{\lambda \sin \alpha}\right) \tag{8}$$

C. THREE-STEP GROWTH

Another possible model of island growth is a three-step mechanism in which islands of a constant lateral dimension w_0 grow to a certain thickness h, then grow at that thickness laterally until they coalesce (Fig. 1c). The islands' thickness in this model is independent of their number density on the surface, unlike the case for the two-step model, since lateral and perpendicular dimensions are now independently variable. The initial width w_0 of the islands is limited by ρ, since w_0 must be less than $1/\sqrt{\rho}$ or the islands will cover the entire surface in step 1 and growth will simply be layer by layer. Again, no new nuclei are formed during deposition.

During the first stage of growth, the area covered by the deposit per unit area of substrate is simply $A = w_0^2 \rho$, so

$$\frac{I(sub)}{I_0(sub)} = w_0^2 \rho \exp\left(- \frac{t}{\lambda \sin \alpha}\right) + \left(1 - w_0^2 \rho\right) \tag{9}$$

The average thickness of the deposit $s = t\, w_0^2 \rho$, so

$$\frac{I(sub)}{I_0(sub)} = 1 + w_0^2 \rho \left[\exp\left(- \frac{s}{w_0^2 \rho \lambda \sin \alpha}\right) - 1\right] \tag{10}$$

This growth phase applies for $0 < s < h w_0^2 \rho$.

In the second step, the islands maintain a thickness h and spread laterally until they coalesce. This step occurs for $h w_0^2 \rho < s < h$. The substrate intensity ratio can be expressed as

8

$$\frac{I(\text{sub})}{I_0(\text{sub})} = \frac{I}{I_0} \text{ (covered after step 1)} + \frac{I}{I_0} \text{ (covered during step 2)}$$

$$+ \frac{I}{I_0} \text{ (not covered)}$$

$$= w_0^2 \rho \exp\left(- \frac{h}{\lambda \sin \alpha}\right) + \left[\exp\left(- \frac{h}{\lambda \sin \alpha}\right)\right] \left[w^2 \rho - w_0^2 \rho\right] + 1 - w^2 \rho$$

$$= 1 + \frac{s}{h} \left[\exp\left(- \frac{h}{\lambda \sin \alpha}\right) - 1\right] \tag{11}$$

Finally, after coalescence ($s > h$)

$$\frac{I(\text{sub})}{I_0(\text{sub})} = \exp\left(- \frac{s}{\lambda \sin \alpha}\right) \tag{12}$$

For the deposit intensity ratio in the first step of growth ($0 < s < h w_0^2 \rho$), we obtain

$$\frac{I(\text{dep})}{I_0(\text{dep})} = w_0^2 \rho \left[1 - \exp\left(- \frac{s}{w_0^2 \rho \lambda \sin \alpha}\right)\right] \tag{13}$$

In the second step ($h w_0^2 \rho < s < h$)

$$\frac{I(\text{dep})}{I_0(\text{dep})} = \frac{I}{I_0} \text{ (covered after step 1)} + \frac{I}{I_0} \text{ (covered during step 2)}$$

$$= w_0^2 \rho \left[1 - \exp\left(- \frac{h}{\lambda \sin \alpha}\right)\right] + \left[1 - \exp\left(- \frac{h}{\lambda \sin \alpha}\right)\right] \left[w_0 \rho - w^2 \rho\right]$$

$$= \frac{s}{h} \left[1 - \exp\left(- \frac{h}{\lambda \sin \alpha}\right)\right] \tag{14}$$

After coalescence ($s > h$)

$$\frac{I(\text{dep})}{I_0(\text{dep})} = 1 - \exp\left(- \frac{s}{\lambda \sin \alpha}\right) \tag{15}$$

III. GROWTH MODEL PREDICTIONS

All three growth models produce distinctively different predictions of
signal-intensity ratio variation with average deposit thickness. In this
section, the predictions of each model will be examined for selected
parameters, and then compared with the predictions of the other models.

Figures 2 and 3 show the results of the two-step growth model for
$\lambda \sin\alpha = 4$ Å and $\lambda \sin\alpha = 15$ Å, respectively. The two-step model produces the
dotted curves, and for comparison the one-step model (layer-by-layer growth)
is given as the solid line. The intensity ratio predicted by the two-step
model can be much larger than that predicted for layer-by-layer growth: i.e.,
the clumping of material in islands allows more electrons from the substrate
to escape than would the spreading of the same amount of material over the
substrate in smooth layers. After coalescence, of course, the one- and two-
step models predict the same behavior. If few islands are present initially,
they must grow taller before coalescing than if the islands are more
numerous. Thus, for larger t_0, coalescence takes place at larger average
thicknesses. Also, islands that are fewer and taller are less effective than
more numerous, shorter islands in preventing the escape of substrate elec-
trons, so the intensity ratio falls off more slowly for large t_0 than for
small t_0. This can be seen very clearly in Fig. 4, in which $t_0 = 32$ Å implies
an initial number density of islands (ρ) of 0.001 Å^{-2}, and $t_0 = 10$ Å implies
$\rho = 0.01$ Å^{-2}. Comparison of Figs. 2 and 3 shows that increasing the escape
depth of the electrons causes the intensity ratio to fall off more slowly,
since the measurement is now less sensitive to the surface structure.

The two-step growth model predicts a slower rise in the intensity ratio
for the deposit than does the one-step model. In Fig. 5 it can be seen
clearly that numerous short islands approach layer-by-layer behavior more
closely than do fewer taller islands.

The three-step growth model is similar to the two-step growth model in
predicting a slower decrease in substrate intensity ratio than the one-step

PREVIOUS PAGE
IS BLANK
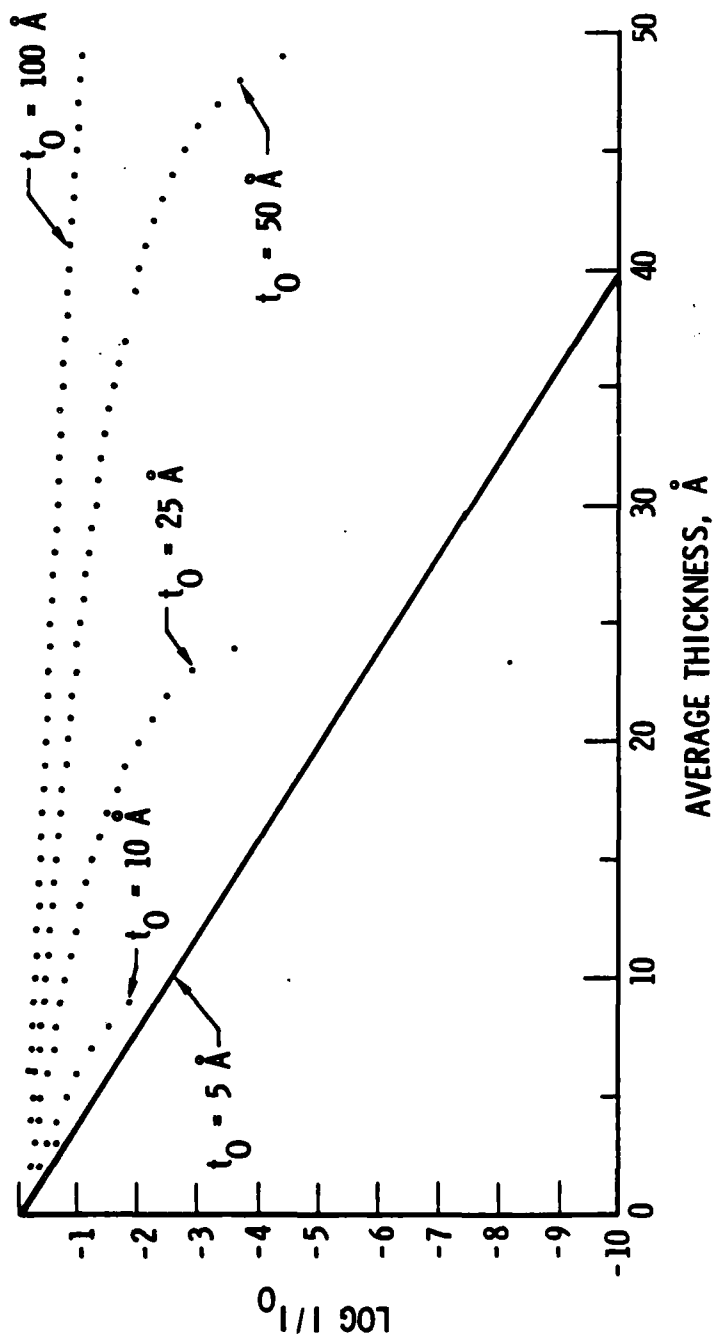
Fig. 2. Results of the Two-Step Model for Substrate Intensity Ratio for λsinα = 4 Å and Various Values of t_0. The solid line is the result for the one-step model.

12

Fig. 3. Results of the Two-Step Model for Substrate Intensity Ratio for $\lambda \sin\alpha = 15$ Å and Various Values of t_0. The solid line is the result for the one-step model.

13

Fig. 4. Results of the Two-Step Model for Substrate Intensity Ratio for Small Average Thickness of Deposit

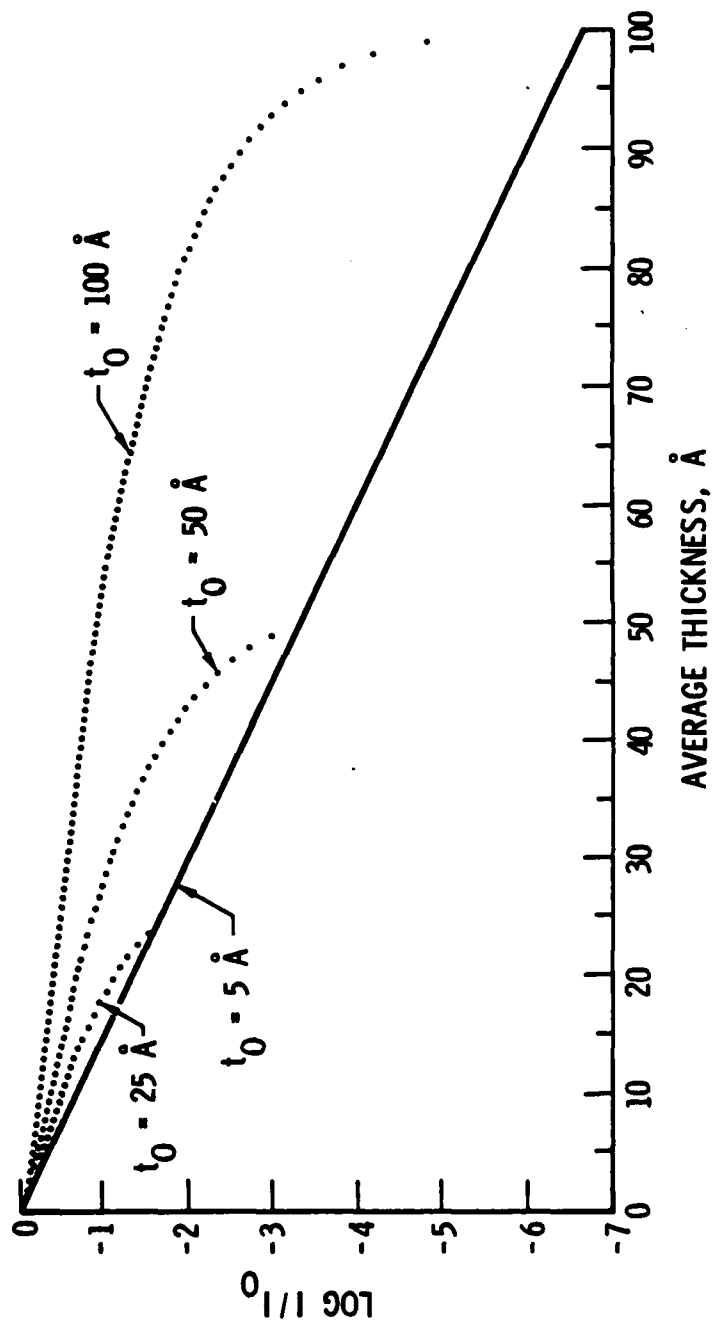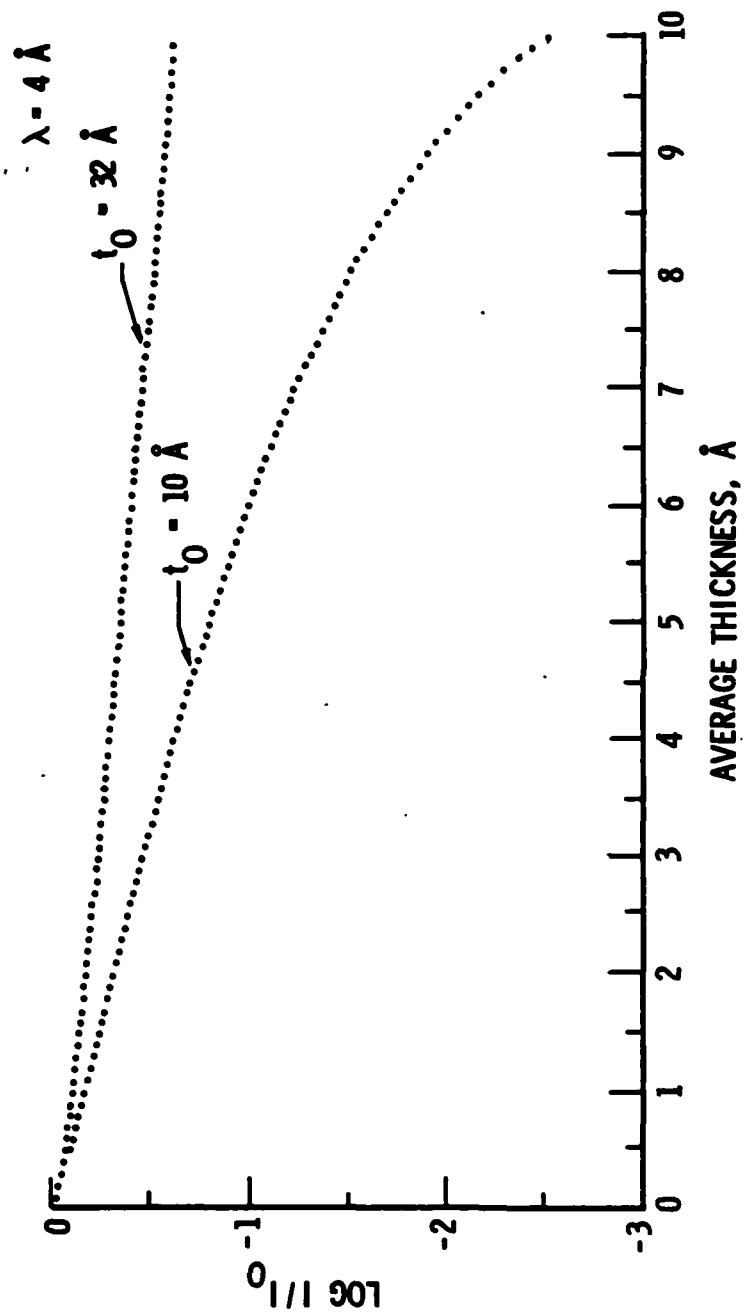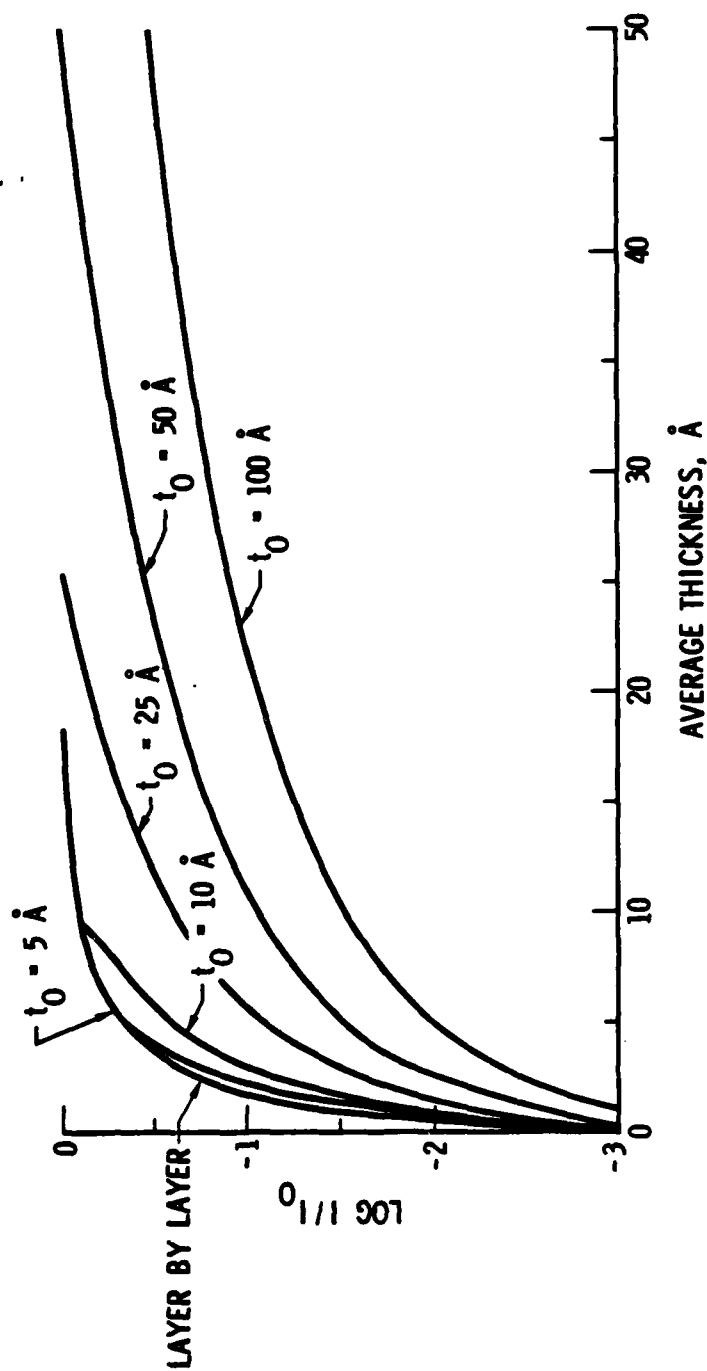Fig. 5. Results of the Two-Step Model for Deposit Intensity Ratio for $\lambda\sin\alpha = 4$ Å and Various Values of t_0

15

growth model (Fig. 6). This figure also illustrates that for the same number density of islands with the same lateral dimension on the surface (the same ρ and w), shorter islands (smaller h) are more effective in removing substrate electrons than are taller islands, since they reach steps 2 and 3 of growth for less material deposited (smaller s). By comparing Figs. 6 and 7, one can see that broader islands (larger w) cause the substrate intensity ratio to decrease more rapidly than do smaller islands. A similar effect obtains for an increase in the number density of islands. Just as in the two-step model, the more the material that is "wasted" by clumping into islands, the slower the decrease in the substrate intensity ratio.

A major difference between the two- and three-step models can be seen by examination of Figs. 4 and 8. The shapes predicted for the intensity ratio curves by the two models for small average thickness of deposit are very different. For the two-step model, $t_0 = 10$ Å implies an initial number density of islands of 0.01 Å^{-2}, and islands that are 10 Å high and 10×10 Å in lateral dimension at coalescence, while $t_0 = 32$ Å implies $\rho = 0.001$ Å^{-2}. The three-step model curves are given for $\rho = 0.001$ Å^2 and $w = 10$ Å. For a wide range of h values, no three-step curve approximates the two-step curve. Because of the very different functional forms of Eqs. (5) and (10), the two-step model will always predict a flatter behavior for the substrate intensity ratio decrease in the initial stages of deposition. The two-step model has a dependence on average thickness s that behaves as $s^{2/3} \exp(-s^{1/3})$. The three-step model predicts a substrate ratio decrease of a shape given by $\exp(-s)$, which initially will fall more rapidly than the two-step model prediction. This difference in the models' predictions becomes very important when comparing the models to experimental data.

The intensity ratio increase for the deposit as a function of average deposit thickness is given in Fig. 9 for $\rho = 0.001$ Å^{-2}, $\lambda = 4$ Å, $w = 10$ Å, and several values of h. Overall, the predictions of the two- and three-step models are similar except in the region of very small deposit thickness, where the differences between the models are most noticeable.
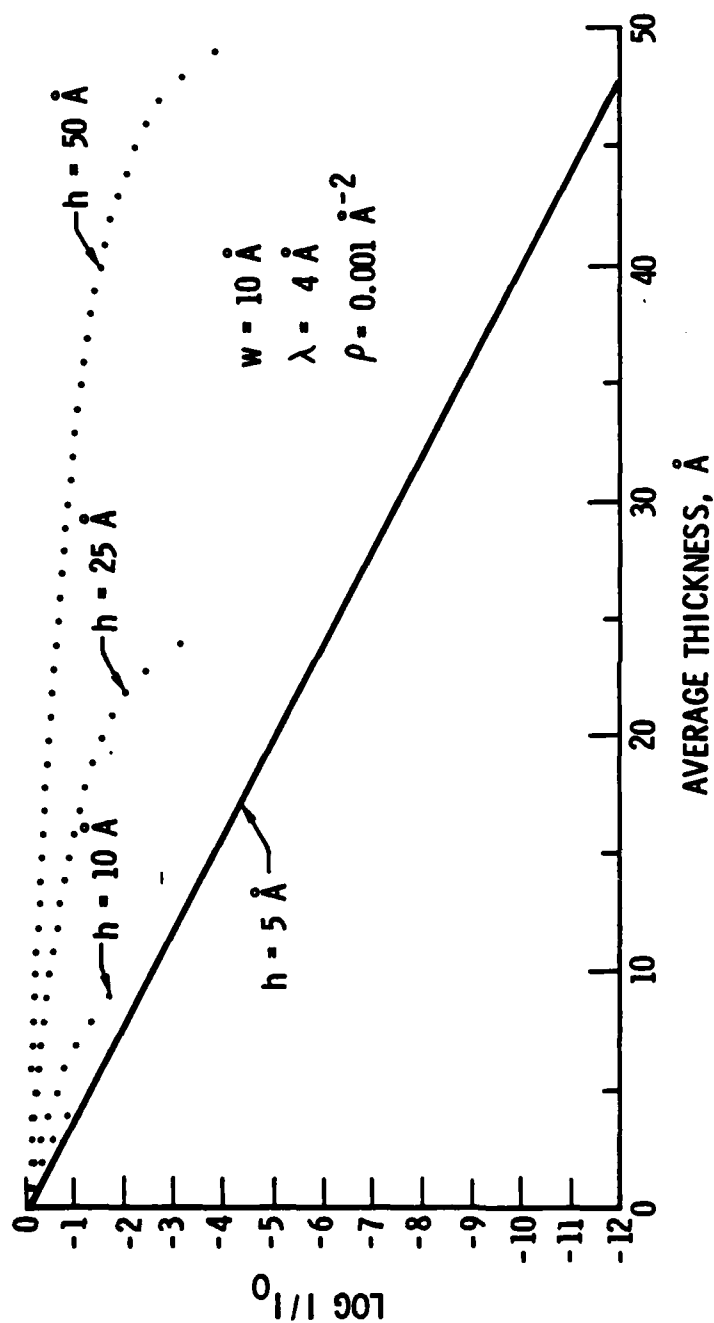
Fig. 6. Results of the Three-Step Model for Substrate Intensity Ratio for $\lambda \sin \alpha$ 4 Å, Island Width w = 10 Å, Island Number Density ρ = 0.001 Å^{-2}, and Various Values of Island Height when Lateral Growth Begins. The solid line is the result for the one-step model.

17

Fig. 7. Results of the Three-Step Model for Substrate Intensity Ratio for the Same Parameter Values as Used in Fig. 6, except for Island Width w = 25 Å. The solid line is the result for the one-step model.
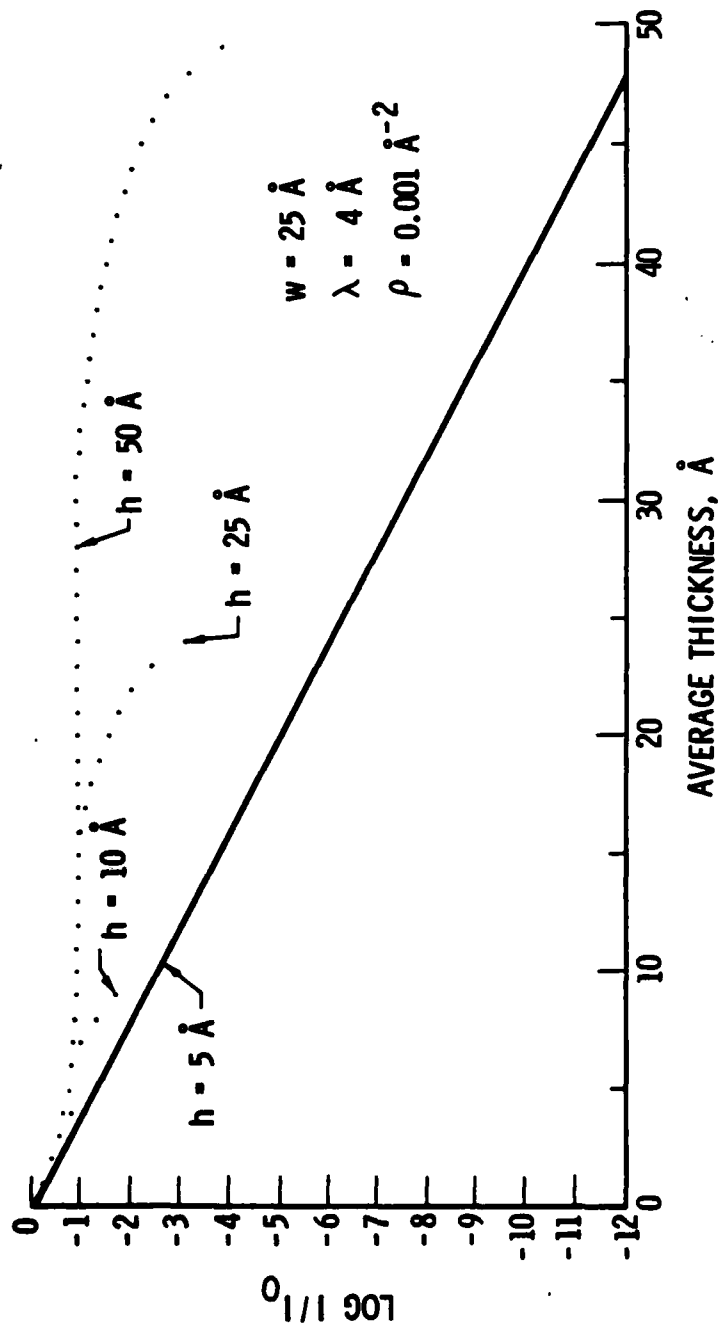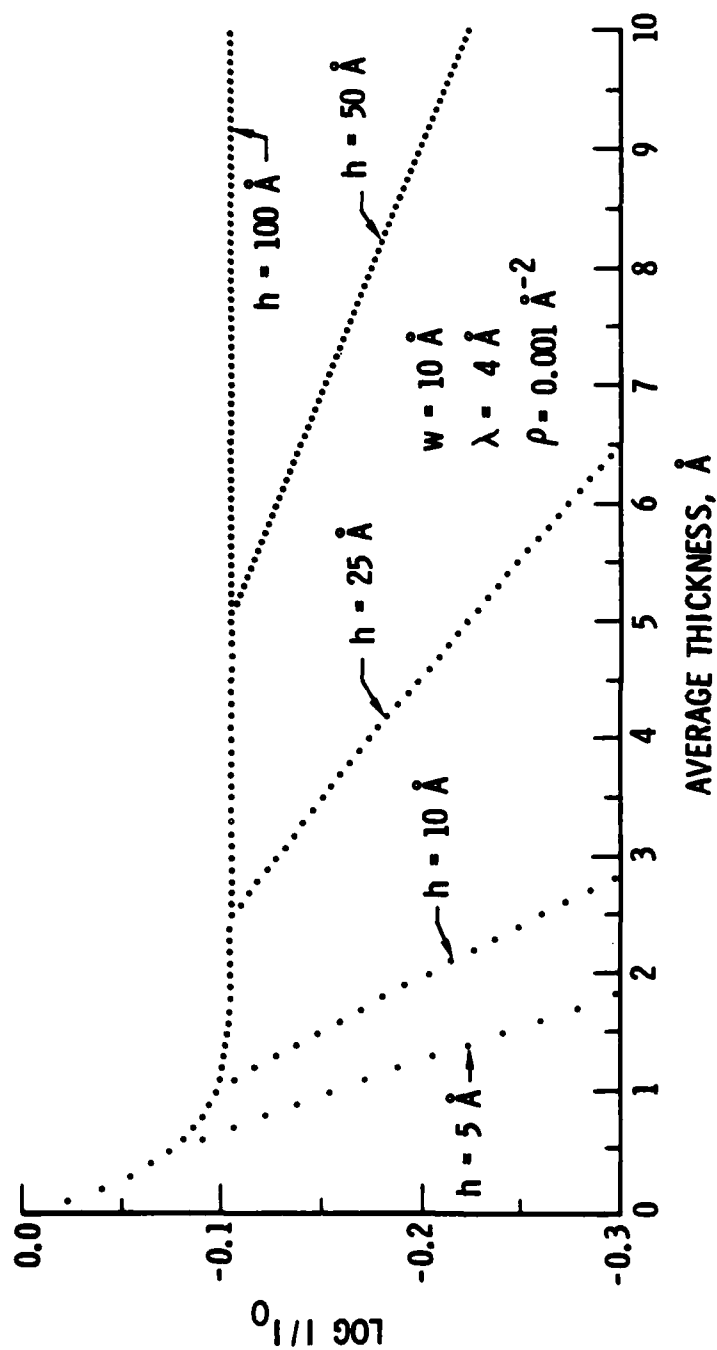
18

Fig. 8. Results of the Three-Step Model for Substrate Intensity Ratio for the Same Parameter Values as Used in Fig. 6, for a Small Average Thickness of Deposit
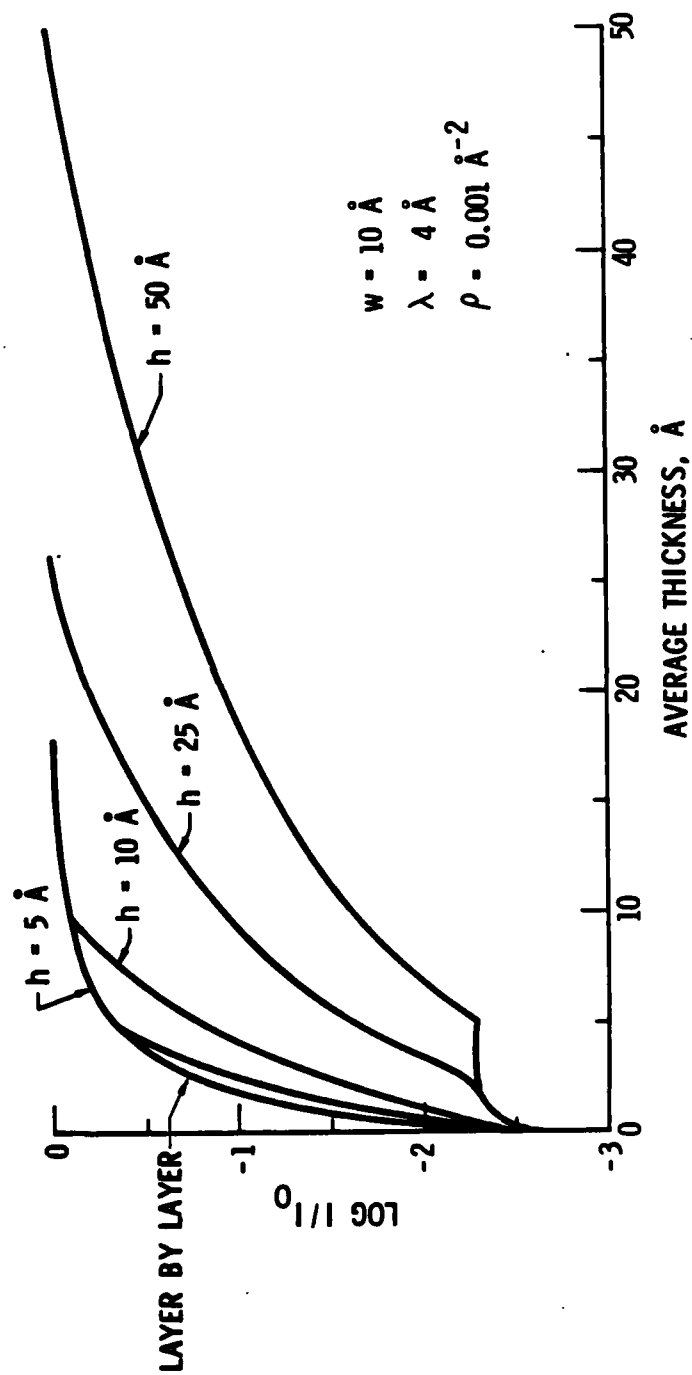
Fig. 9. Results of The Three-Step Model for Deposit Intensity Ratio for the Same Parameter Values as Used in Fig. 6

20

IV. COMPARISON OF MODELS TO EXPERIMENT

Rossi et al.[1] studied the deposition of Ag on Ge by using UPS from a synchrotron radiation source. The escape depth for the analyzed electrons was estimated to be 5 Å for both the Ag and Ge photoelectrons. The data for the intensity-ratio change of the deposit signal with average deposit thickness was arbitrarily normalized to its value for the smallest average thickness in the original work and is arbitrarily renormalized for comparison to the models presented here. The data for the substrate signal was normalized properly to the signal intensity before deposition, so a quantitative comparison to the models is possible in this case.

Figures 10 and 11 show the predictions of the two-step growth model for three choices of t_0 (solid curves) compared to the experimental data (dots). The substrate intensity ratio is not well fit by this model (Fig. 10). For many small islands ($t_0 = 3$ Å), the model predicts a too-rapid decrease in substrate intensity. For fewer larger islands, the intensity ratio does not fall rapidly enough for small amounts of deposit, and falls too rapidly for larger amounts. However, the deposit signal intensity ratio can be fit quite well by the two-step model. In Fig. 11 the experimental data have been arbitrarily renormalized to fit the $t_0 = 25$ Å prediction, but different renormalization would enable the data to fit the other curves as well. Thus the ability to use deposit signal intensity data to distinguish between growth models is extremely limited.

The three-step growth model fits the substrate intensity ratio data very well (Fig. 12). This is not a simple consequence of the fact that the three-step model contains more parameters than the two-step model. The shape of the three-step model's predicted form, which is determined by the growth mode, is the key factor. The parameters chosen for the model are all reasonable: Islands 25 Å wide grow to a height of 40 Å (or more) before spreading to cover the surface. Coalescence had not yet occurred for these parameters by the average thickness of 25 Å, when the experiment was terminated. As can be seen in Fig. 7, there will be a sharp downturn in the predicted intensity

Fig. 10. Comparison of the Two-Step Model (solid curves) with Experimental Data for Ag Deposition on Ge (dots) for Substrate Intensity Ratio

22

Fig. 11. Comparison of the Two-Step Model (solid curves) with Experimental Data for Ag Deposition on Ge (dots) for Deposit Intensity Ratio

23

$w = 25$ Å
$\lambda = 5$ Å
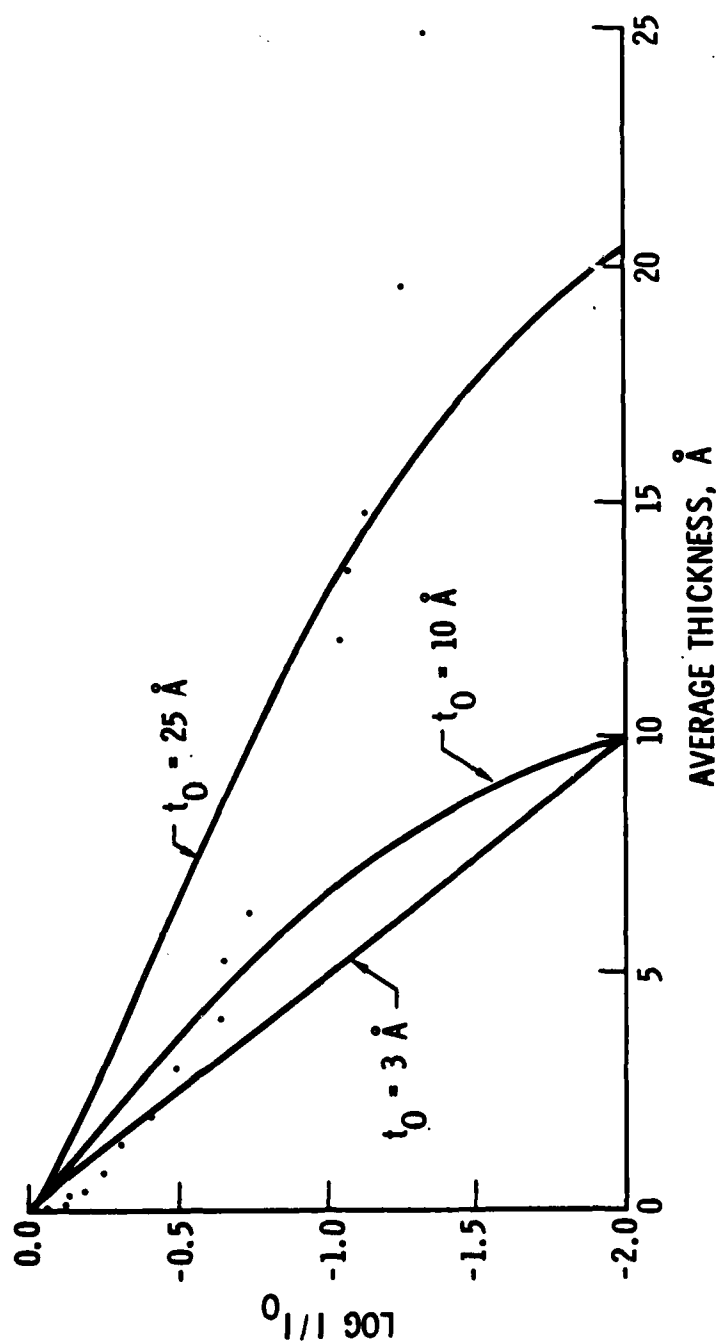$\rho = 0.001$ Å^{-2}
$h = 40$ Å

AVERAGE THICKNESS, Å

LOG I/I_0
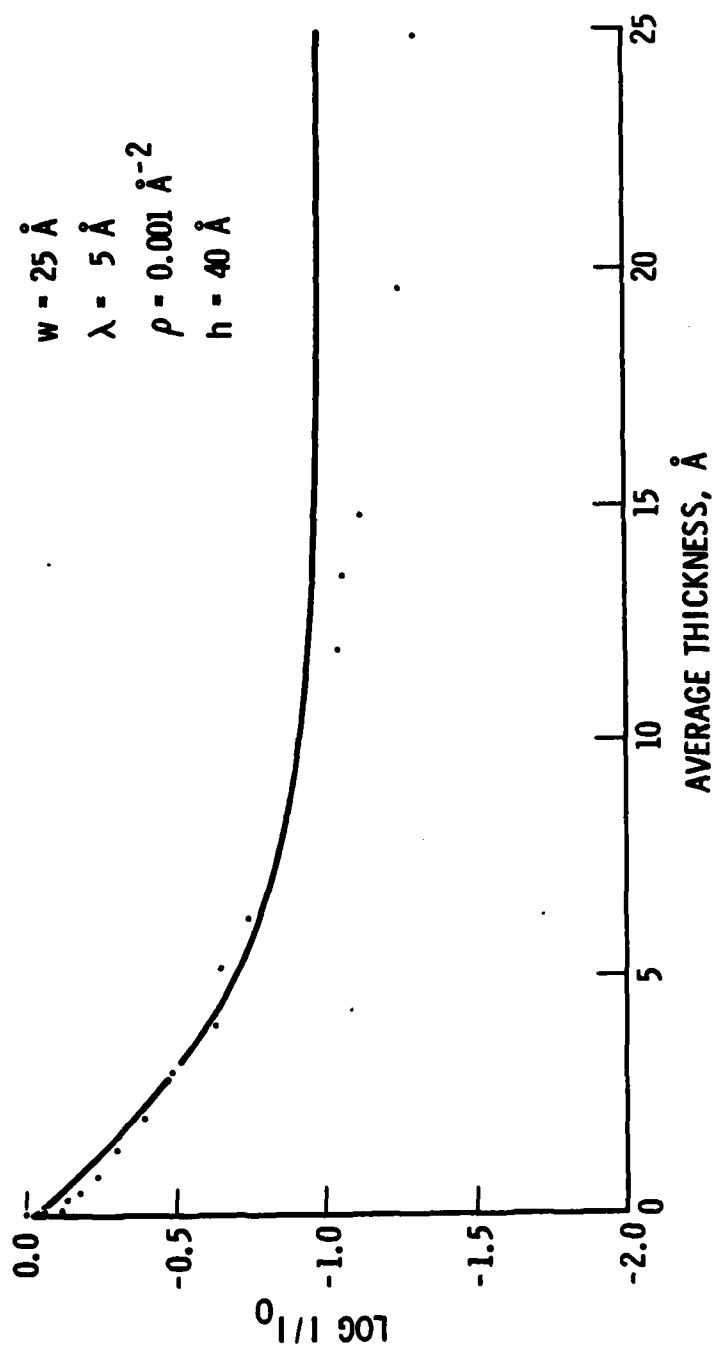
Fig. 12. Comparison of the Three-Step Model (solid curve) with
Experimental Data for Ag Deposition on Ge (dots) for
Substrate Intensity Ratio

at ~ 35 Å, followed by layer-by-layer growth at 40 Å, if the islands indeed grow to be 40 Å tall. Taller islands (larger h) will not affect the fit in the region for which data are available, but the transitions between steps will shift to larger average thickness. The three-step model also fits the deposit intensity ratio well (Fig. 13), but, as discussed above, this is not very conclusive. The important distinction between the two models is that the three-step model fits the substrate intensity ratio data, while the two-step model does not.
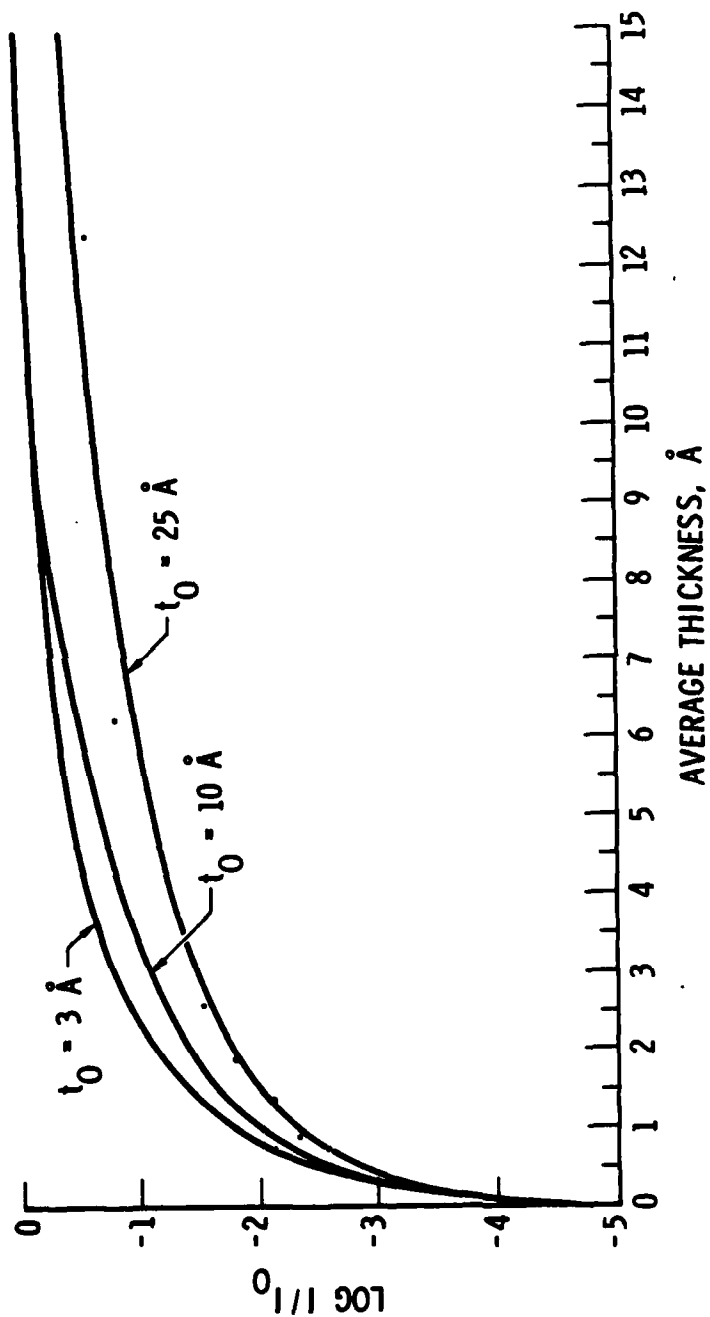
Fig. 13. Comparison of the Three-Step Model (solid curve) with Experimental Data for Ag Deposition on Ge (dots) for Deposit Intensity Ratio
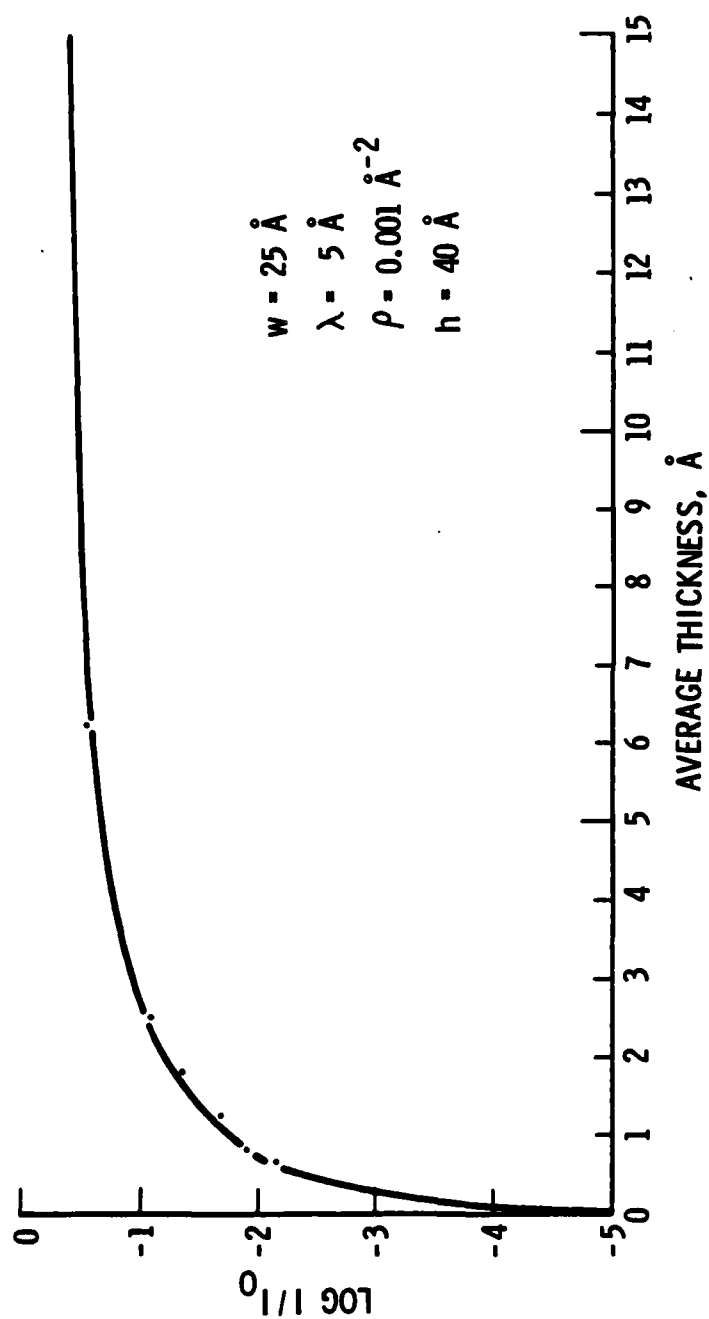
V. CONCLUSIONS

The growth mode of thin-film deposition must be taken into account when
one assesses surface electron spectroscopy data for evidence of interdiffusion
of deposit and substrate material at early stages of deposition. It has been
shown here that island growth mechanisms predict very different substrate and
deposit signal intensity trends with increasing deposit thickness than does
the simple often-assumed layer-by-layer growth mechanism. When deposited
material clumps into islands, it is less effective at shielding substrate
electrons from detection than it would be were it spread evenly over the
surface. This slower-than-expected decrease in substrate intensity could
be mistakenly interpreted as the diffusion of substrate atoms through the
deposit. Similarly, the slower-than-expected increase in deposit intensity
could be mistakenly interpreted as the diffusion of deposited atoms into the
substrate. More data, such as valence-band shape changes in UPS, or scanning
or transmission electron micrographs verifying the deposit growth mode, must
be obtained before conclusions concerning diffusion vs. island formation can
be made.

In this report, two models of island growth have been examined and
compared to experimental data obtained for Ag deposition on Ge. The two-step
growth model, in which island growth perpendicular to the surface occurs at
the same rate as lateral island growth, was shown not to fit the experimental
data. The three-step model, in which islands of a fixed lateral dimension
first grow to a given height and then spread to cover the surface, was shown
to fit the data very well. This does not prove that interdiffusion of Ag and
Ge cannot also account for the data, but it does show that more information is
needed to address that question. The influence of the mode of deposit growth,
particularly island growth, must not be neglected in the application of
surface electron spectroscopies to thin-film phenomena.

REFERENCES

1. G. Rossi, I. Abbati, L. Braicovich, I. Lindau, and W. E. Spicer, _Phys. Rev. B_ _25_, 3619 (1982).

2. R. Ludeke, _Surface Sci._ _132_, 143 (1983).

3. W. H. Makky, F. Cabrera, K. M. Geib, and C. W. Wilmsen, _J. Vac. Sci. Technol._ _21_, 417 (1982).

4. V. I. Nefedov, _Surf. Interf. Anal._ _3_, 72 (1981).

PREVIOUS PAGE
IS BLANK

LABORATORY OPERATIONS

The Laboratory Operations of The Aerospace Corporation is conducting experimental and theoretical investigations necessary for the evaluation and application of scientific advances to new military space systems. Versatility and flexibility have been developed to a high degree by the laboratory personnel in dealing with the many problems encountered in the nation's rapidly developing space systems. Expertise in the latest scientific developments is vital to the accomplishment of tasks related to these problems. The laboratories that contribute to this research are:

Aerophysics Laboratory: Launch vehicle and reentry aerodynamics and heat transfer, propulsion chemistry and fluid mechanics, structural mechanics, flight dynamics; high-temperature thermomechanics, gas kinetics and radiation; research in environmental chemistry and contamination; cw and pulsed chemical laser development including chemical kinetics, spectroscopy, optical resonators and beam pointing, atmospheric propagation, laser effects and countermeasures.

Chemistry and Physics Laboratory: Atmospheric chemical reactions, atmospheric optics, light scattering, state-specific chemical reactions and radiation transport in rocket plumes, applied laser spectroscopy, laser chemistry, battery electrochemistry, space vacuum and radiation effects on materials, lubrication and surface phenomena, thermionic emission, photosensitive materials and detectors, atomic frequency standards, and bioenvironmental research and monitoring.

Electronics Research Laboratory: Microelectronics, GaAs low-noise and power devices, semiconductor lasers, electromagnetic and optical propagation phenomena, quantum electronics, laser communications, lidar, and electro-optics; communication sciences, applied electronics, semiconductor crystal and device physics, radiometric imaging; millimeter-wave and microwave technology.

Information Sciences Research Office: Program verification, program translation, performance-sensitive system design, distributed architectures for spaceborne computers, fault-tolerant computer systems, artificial intelligence, and microelectronics applications.

Materials Sciences Laboratory: Development of new materials: metal matrix composites, polymers, and new forms of carbon; component failure analysis and reliability; fracture mechanics and stress corrosion; evaluation of materials in space environment; materials performance in space transportation systems; analysis of systems vulnerability and survivability in enemy-induced environments.

Space Sciences Laboratory: Atmospheric and ionospheric physics, radiation from the atmosphere, density and composition of the upper atmosphere, aurorae and airglow; magnetospheric physics, cosmic rays, generation and propagation of plasma waves in the magnetosphere; solar physics, infrared astronomy; the effects of nuclear explosions, magnetic storms, and solar activity on the earth's atmosphere, ionosphere, and magnetosphere; the effects of optical, electromagnetic, and particulate radiations in space on space systems.

END

FILMED

10-84

DTIC